Supplemental Materials and Methods

Time-resolved FRET (trFRET) to probe for changes in the Box A/A' stem upon complex assembly

U3 MINI was folded and the decay of Fl fluorescence was measured at 20 °C (see below) for 0.5 μM solutions of either singly (Fl-U3 MINI) or doubly (Fl-U3 MINI-Rh, manuscript Fig. 4b) labeled U3 MINI in reaction buffer. Measurements were made either in the absence or presence of protein and/or the 18S site RNA with a final volume of 80 μl. For the binary complex, Imp3p in reaction buffer was added to a final concentration of 1 μM and incubated for ~15 min. For the ternary chaperone complex, Imp4p was added to a preformed binary complex with a final concentration of 1.5 μM and incubated for ~15 min. Finally, 18S in reaction buffer was added at a final concentration of 0.5 μM to a preformed chaperone complex, and the fluorescence decay measured.

Time-resolved donor fluorescence decays (Fig. S1) were collected using time-correlated single-photon counting, as described previously[1,2]. A frequency-doubled Nd:YVO_4 laser (Spectra-Physics Millenia Xs, with LBO doubling crystal, operated at 9.0 W) pumped a mode-locked Ti:Sapphire laser (Spectra-Physics Tsunami, Spectra-Physics, Mountain View, CA, USA) giving ~600 mW output power, which was frequency-doubled to excite Fl at 490 nm. The output pulse width was 2 ps, and the pulse repetition rate was picked down to 4 MHz. A microchannel plate photomultiplier tube (Hamamatsu R3809U-50, Hamamatsu, Bridgewater, NJ, USA) in conjunction with a SPC-630 time correlated single-photon counting card (Becker & Hickl, Berlin, Germany) was used to collect isotropic emission at 520 nm (Chroma 10-nm bandpass interference filter, Chroma, Rockingham, VT, USA) into 4,096 sampling channels with a time increment of 12.2 ps/channel. Photons were collected under magic angle polarizer conditions, with peak counts ranging from 20,000 to 40,000 counts. Instrument response

functions were measured from the scattered signal of a dilute solution of nondairy coffee creamer and convoluted with an intensity decay model, discussed below, and used in conjunction with a Levenberg-Marquardt nonlinear least-squares fit to deconvolute the sample decay curves.

To measure donor-acceptor distances, time-resolved fluorescence decays of each sample were collected with and without acceptor in place. The difference in the fluorescein decay of the singly and corresponding doubly labeled samples was utilized to extract three-dimensional Gaussian distance distributions between the two fluorophores as previously described[1,2]. The fluorescein emission amplitudes α_i and lifetimes τ_i of the singly labeled samples were determined by a fit to a sum of 3 exponentials and a constant (Supplemental Fig. S1). The donor decay of the ensemble of flexible donor-acceptor pairs was modeled as a weighted average of the decays for each donor-acceptor distance modeled by

$$I_{DA}(t) = \sum_k f_k \int P_k(R) \sum_i \alpha_i \exp\{-\frac{t}{\tau_i}[1 + (\frac{R_o}{R})^6]\} dR \qquad \text{(S1)}$$

where $P_k(R) = 4\pi R^2 c \exp[-a(R-b)^2]$ is a three-dimensional Gaussian distribution, in which a and b are parameters that describe the shape of the distribution and c is a normalization constant. A value of 54 Å was used for the Förster distance R_0 between Fl and Rh under the assumption of free isotropic rotation of the two dyes[1,2].

Derivation of equations for non-pseudo first-order kinetics and half-life for hybridization

The following analysis is adapted from Malatesta[3]. Duplex formation can be represented by

$$A + B \underset{k_{off}}{\overset{k_{on}}{\rightleftharpoons}} AB \qquad \text{(S2)}$$

where A and B represent the two complementary nucleic acid strands. The overall rate equation

$$\frac{d[AB]}{dt} = k_{on}[A][B] - k_{off}[AB] \quad \text{(S3)}$$

where *[A]*, *[B]* and *[AB]* are concentrations at any time t. If we assume that *x* reflects the concentration of AB and that at initial time *[AB]* = 0, then

$$\frac{dx}{dt} = k_{on}(A_0 - x)(B_0 - x) - k_{off}x \quad \text{(S4)}$$

$$= k_{on}A_0B_0 + x(-k_{on}A_0 - k_{on}B_0 - k_{off}) + k_{on}x^2 \quad \text{(S5)}$$

let $a = k_{on}$ (S6a)

$b = -(k_{on}A_0 + k_{on}B_0 + k_{off})$ (S6b)

$c = k_{on}A_0B_0$ (S6c)

which rearranges to

$$\int \frac{dx}{ax^2 + bx + c} = \int dt \quad \text{(S7)}$$

Definite integration of S7 yields

$$\frac{1}{\sqrt{b^2 - 4ac}} \ln\left\{\frac{2ax + b - \sqrt{b^2 - 4ac}}{2ax + b + \sqrt{b^2 - 4ac}}\right\}\Bigg|_0^x = t\Big|_0^t = t \quad \text{(S8)}$$

Equation S8 simplifies to

$$x = x_{eq}\frac{[1 - e^{-zt}]}{[1 + we^{-zt}]} \quad \text{(S9)}$$

where $z = \sqrt{k_{on}^2(A_0 - B_0)^2 + 2k_{on}k_{off}(A_0 + B_0) + k_{off}^2}$ (S10a)

$$w = \frac{-(b + z)}{(b - z)} \quad \text{(S10b)}$$

$$x_{eq} = \frac{-(b + z)}{2k_{on}} \quad \text{(S10c)}$$

For ideal FRET conditions $A_0 = B_0$, which simplifies equations S5b and S9a to

$b = -(2k_{on}A_0 + k_{off})$ (S11)

$$z = \sqrt{4k_{on}k_{off}A_0 + k_{off}^2} \quad \text{(S12)}$$

The half-life for hybridization is the time it takes half of the single stranded substrates to be converted into duplex. To solve for the half-life $t_{1/2}$ set $\frac{x}{x_{eq}} = 0.5$ and solve for t

$$0.5 = \frac{[1 - e^{-zt}]}{[1 + we^{-zt}]} \quad \text{(S13)}$$

that simplifies to

$$t_{1/2} = \frac{1}{z}\ln(2 - \frac{b+z}{b-z}) \quad \text{(S14)}$$

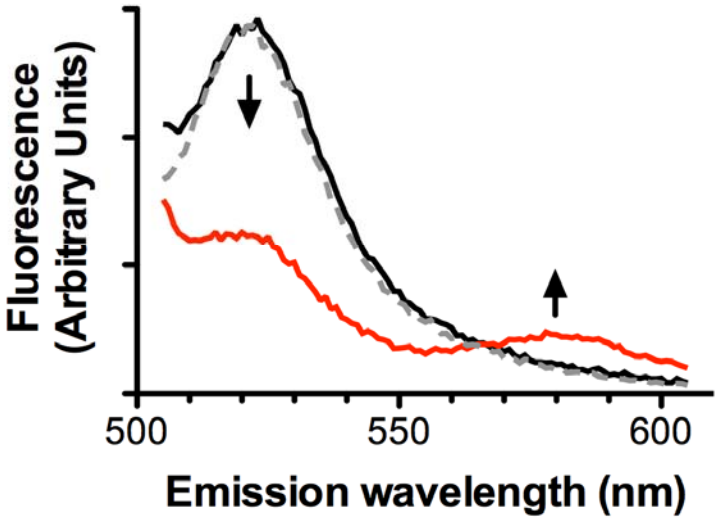

Fig. S1. FRET signal associated with U3-18S duplex formation. An emission spectrum of 5 nM Fl-U3 MINI in the presence of saturating amounts of Imp3p and Imp4p before (black) and after addition of 5 nM 18S-Rh (red). The before and after spectra were normalized to account for dilution. Addition of acceptor containing RNA molecules results in a decrease in Fl emission (down arrow) with the concomitant increase in Rh emission (up arrow), consistent with a FRET signal. The similarity between the emission spectra before addition of labeled 18S (black) and after addition of 5nM unlabeled 18S to 5 nM Fl-U3 MINI in the presence of saturating amounts of Imp3p and Imp4p (grey dashed line) suggests that the observed signal upon addition of 18S-Rh arises from FRET.

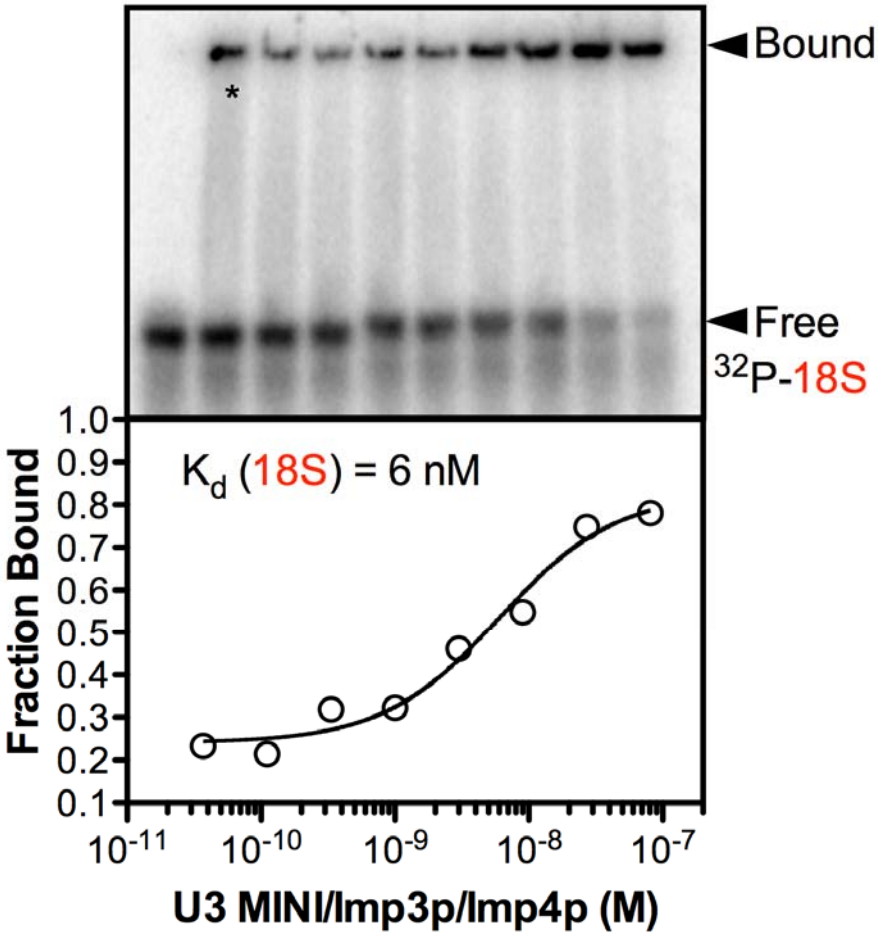

Fig. S2. Representative binding data from electrophoretic mobility shift assays for ^{32}P-18S-U3 MINI in the presence of the saturating amounts of Imp3p and Imp4p. Fraction bound is calculated based on the fraction of ^{32}P-18S shifted and plotted against increasing concentration of the chaperone complex. K_d (18S) is calculated by fitting fraction bound to equation (6) from Material and Methods in the manuscript; the lane marked with an asterisk is an outlier and not used. The mean and standard deviation for three replicas is $(4 \pm 2) \times 10^{-9}$ M.

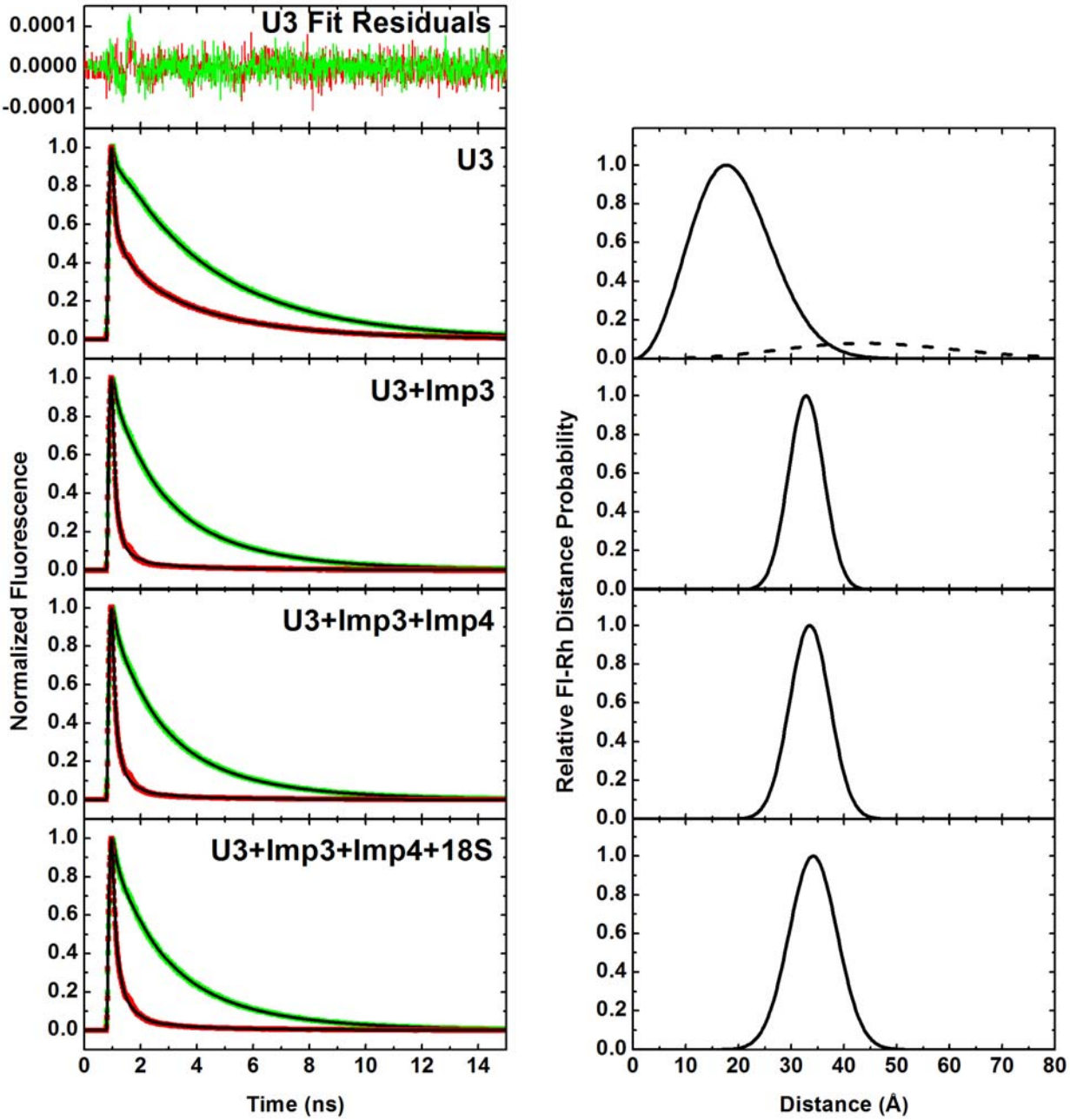

Fig. S3. Time-resolved FRET analysis of the donor-acceptor distance of doubly labeled U3 MINI (main manuscript Fig. 4b), in the presence and absence of Imp3p, Imp4p and 18S. The left column shows the time-resolved fluorescence decay curves for donor only (Fl-U3 MINI, decay data (green) with fits (black)) and donor-acceptor (Fl-U3 MINI-Rh, decay data (red) with fits (black)) doubly labeled U3 MINI for each step of complex formation. The right column shows the corresponding distance distributions as derived from the decay fits by trFRET analysis. Two distance distributions are observed for the U3 MINI alone (solid and dashed lines), whereas single distance distributions are observed for the various U3 MINI chaperone complexes, as discussed in Results. Residuals between the calculated and experimental data are shown for U3 MINI decay curves (upper left panel). Similar residuals are observed for the other decay curves (data not shown).

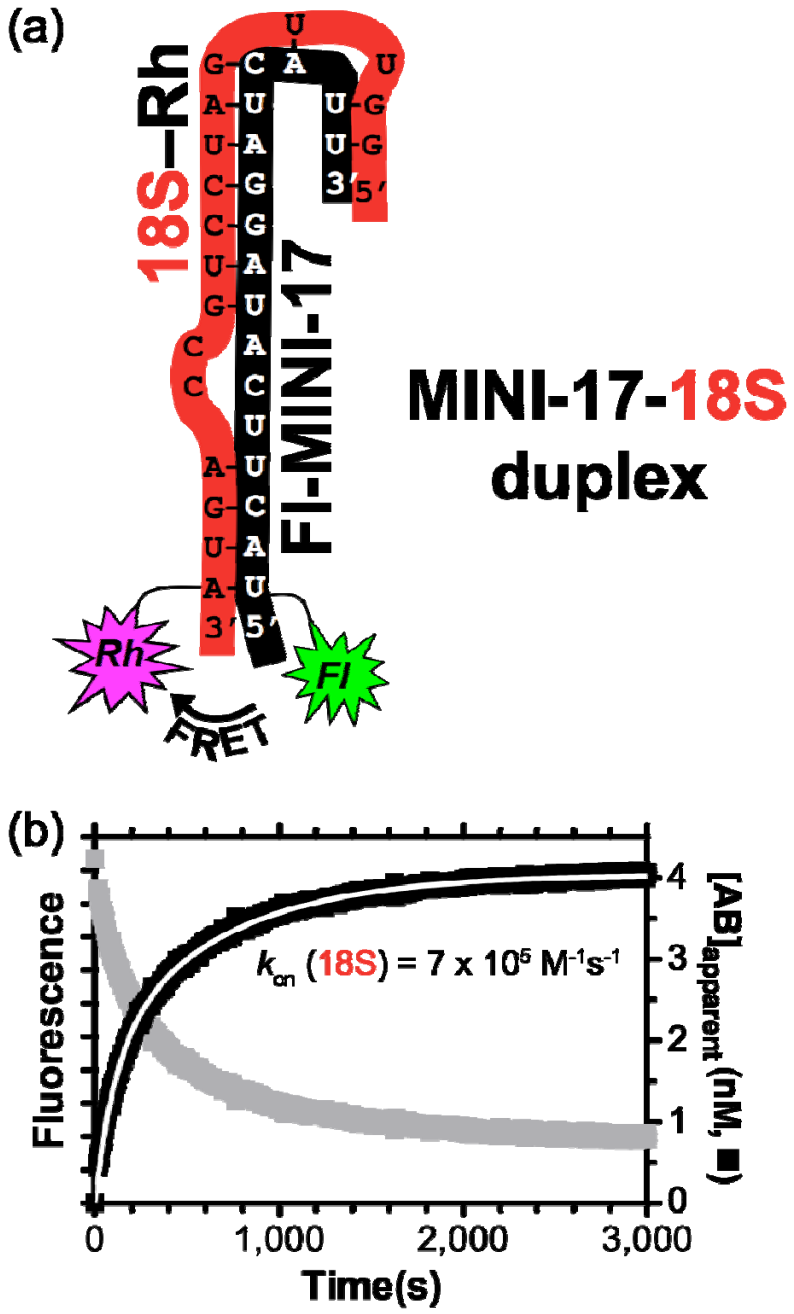

Fig. S4. Hybridization of the MINI-17-18S duplex in the absence of protein. (a) The fluorescently labeled MINI-17-18S duplex substrate used for kinetic measurements includes the donor 5'-Fl labeled MINI-17 (Fl-MINI-17) and the acceptor 3'-Rh labeled 18S (18S-Rh). (b) Raw representative trace (left y-axis, grey points) is shown for fluorescein quenching upon addition of 18S-Rh to Fl-MINI-17 to achieve a final concentration of 5 nM. $[AB]_{apparent}$, calculated using equation (1), is plotted in the right y-axis (black squares) along with the fit (white line) to equation (2a) to give a value of 7 x 10^5 M^{-1} s^{-1} for k_{on} (18S) (the fit was performed using molar $[AB]_{apparent}$). Both equations are from the Materials and Methods of the manuscript.

References for Supplementary Material

1. Pereira, M. J., Harris, D. A., Rueda, D. & Walter, N. G. (2002). Reaction pathway of the trans-acting hepatitis delta virus ribozyme: a conformational change accompanies catalysis. *Biochemistry* **41**, 730-740.
2. Rueda, D., Wick, K., McDowell, S. E. & Walter, N. G. (2003). Diffusely bound Mg2+ ions slightly reorient stems I and II of the hammerhead ribozyme to increase the probability of formation of the catalytic core. *Biochemistry* **42**, 9924-9936.
3. Malatesta, F. (2005). The study of bimolecular reactions under non-pseudo-first order conditions. *Biophys Chem* **116**, 251-256.